*Progress In Electromagnetics Research C, Vol. 47, 139–146, 2014*

# UWB/Omni-Directional Microstrip Monopole Antenna for Microwave Imaging Applications

**Nasser Ojaroudi*, Mohammad Ojaroudi, and Yaser Ebazadeh**

**Abstract**—In this paper, a new design of multi-resonance monopole antenna for use in microwave imaging systems is presented. The antenna configuration consists of an ordinary square radiating patch, a feed-line, and a modified ground plane with pairs of L-shaped slits and parasitic structures which provides a wide usable fractional bandwidth of more than 130% (2.95–14.27 GHz). In the presented design, by cutting a pair of L-shaped slits and also by embedding a pair of inverted L-shaped parasitic structures in the ground plane additional resonances at 9.5 GHz and 13.7 GHz can be achieved. By using these structures, the usable upper frequency of the antenna is extended from 10.3 GHz to 14.27 GHz. The proposed antenna has a symmetrical structure with ordinary square radiating patch, therefore displays good omni-directional radiation patterns even at higher frequencies. The antenna has sufficient and acceptable gain level and also its radiation efficiency is greater than 86% across the entire radiating band. The designed antenna has a small dimension.

## 1. INTRODUCTION

In general, the microwave imaging system is formed by a circular cylindrical array antenna in order to detect cancerous tissue. In this approach, circular cylindrical microwave imaging systems require small antennas with omnidirectional radiation patterns and large bandwidth [1–3]. The majority of the compact ultra-wideband (UWB) antennas presented in the literature exhibit omnidirectional radiation patterns with relatively low gain and an impulse response with observable distortion. These types of UWB antennas are suitable for the short-range indoor and outdoor communication. However, for radar systems, such as a UWB microwave imaging system for detection of tumor in woman's breast, a moderate gain directional antenna is advantageous. Additionally, in order to achieve an UWB impedance bandwidth, as defined by the minimum return loss of the 10 dB, antenna is required to support a very short pulse transmission with negligible distortion. This is necessary to achieve precision imaging without ghost targets.

The unipolar and antipodal Vivaldi antennas presented in the literature [4, 5] satisfy the requirements for imaging systems in terms of bandwidth, gain, and impulse response. However, the achieved performance is at the expense of a significant size, which has a length of several wavelengths. Therefore, the challenge is to reduce their physical dimensions such that it can be incorporated in a compact microwave imaging detection system while maintaining its broadband, high-gain, and distortion-less performance. Several UWB antenna designs with compact size and low distortion have been proposed for the use in the medical imaging systems [6–8]. Each has its own merits and drawbacks. Some of the proposed antennas have a no planar structure, whereas others have low-gain and/or low radiation efficiency.

In microwave imaging systems, breast phantom is placed on a rotary stage with antennas scanning at the side to simulate the human breast in prone position. Breast phantom is rotated for 360 degrees relative to the stationary antennas to simulate a circular antenna array around the breast circumference.

*Received 8 January 2014, Accepted 18 February 2014, Scheduled 19 February 2014*
* Corresponding author: Nasser Ojaroudi (n.ojaroudi@yahoo.com).
The authors are with the Germi Branch, Islamic Azad University, Germi, Iran.

The overall experimental setup is shown in Fig. 1. The UWB antennas are used as the transmitter and receiver of the UWB signals.

A new and simple method for designing a novel and compact microstrip-fed monopole antenna with multiresonance characteristic for microwave imaging system applications has been presented. In this paper, based on defected ground structure (DGS), for bandwidth enhancement a pair of L-shaped slits was cut in the ground plane which generates a new resonance at higher frequencies (9.5 GHz). Also based on electromagnetic coupling theory (ECT), by adding a pair of inverted L-shaped parasitic structures at the air gap distance in the ground plane, forth resonance at 13.7 GHz is excited. By using these modified structures, the usable upper frequency of theproposed monopole is improved from 10.30 GHz to 14.27 GHz. The measured maximum gain of the proposed antenna is around of 3.1–6.2 GHz. The antenna dimension is $12 \times 18 \times 1.6\,\text{mm}^3$.

## 2. ANTENNA DESIGN

The proposed monopole antenna fed by a microstrip line is shown in Fig. 2, which is printed on an FR4 substrate of thickness 1.6 mm. The basic structure of the proposed antenna consists of the square radiating patch, a feed-line and a ground plane. The proposed antenna is connected to a 50 Ω SMA connector for signal transmission. The radiating patch is connected to a feed line of width $W_f$ and length $L_f$. The width of the microstrip feed line is fixed at 2 mm, as shown in Fig. 1. On the other side of the substrate, a conducting ground plane of width $W_{sub}$ and $L_{gnd}$ length is placed.

This work started by choosing the dimensions of the designed antenna. These parameters, including the substrate, is $W_{sub} \times L_{sub} = 12 \times 18\,\text{mm}^2$ or about $0.15\lambda \times 0.25\lambda$ at 4.2 GHz (the first resonance frequency). There is a lot of flexibility in choosing the width of the radiating patch. This parameter mostly affects the antenna bandwidth. As $W$ decreases, so does the antenna bandwidth, and vice versa. Next step, we have to determine the length of the radiating patch $L$. This parameter is approximately $\lambda_{\text{lower}}/4$, where $\lambda_{\text{lower}}$ is the lower bandwidth frequency wavelength. $\lambda_{\text{lower}}$ depends on a number of parameters such as the radiating patch width as well as the thickness and dielectric constant of the substrate on which the antenna is fabricated. Final values of the presented antenna design parameters are specified in Table 1.

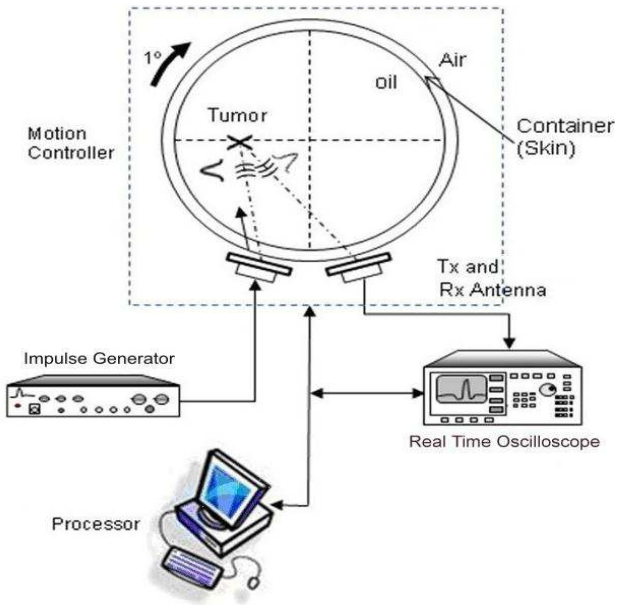


**Figure 1.** Overall experimental setup.

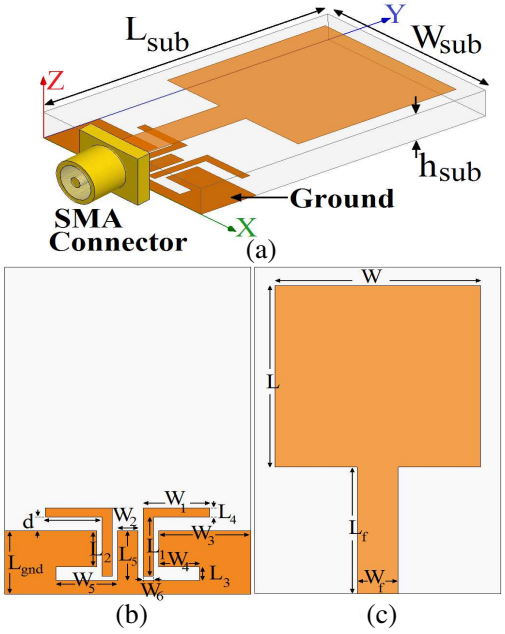


**Figure 2.** Geometry of the proposed antenna, (a) side view, and (b) bottom layer, and (c) top layer.

**Table 1.** Final dimensions of the proposed antenna.

| Param. | mm | Param. | mm | Param. | mm | Param. | mm | Param. | mm |
|---|---|---|---|---|---|---|---|---|---|
| $W_{sub}$ | 12 | $L_{sub}$ | 18 | $h_{sub}$ | 1.6 | $W_f$ | 2 | $L_f$ | 7 |
| $W$ | 10 | $L$ | 10 | $W_1$ | 3.25 | $L_1$ | 3.5 | $W_2$ | 1 |
| $L_2$ | 2 | $W_3$ | 4.5 | $L_3$ | 0.75 | $W_4$ | 1.5 | $L_4$ | 0.5 |
| $W_5$ | 2.5 | $L_5$ | 2.75 | $W_6$ | 0.5 | $L_{gnd}$ | 3.5 | $d$ | 1 |

Regarding DGS theory, the creating slits in the ground plane provide additional current paths. Moreover, these structures change the inductance and capacitance of the input impedance, which in turn leads to change the bandwidth [4, 5]. Therefore, by cutting a pair of L-shaped slits in the ground plane, much enhanced impedance bandwidth may be achieved. In addition, based on ECT, by adding a pair of inverted L-shaped conductor-backed plane in the air gap distance, additional coupling is introduced between the bottom edge of the square patch and the ground plane and its impedance bandwidth is improved without any cost of size or expense.

## 3. RESULTS AND DISCUSSIONS

In this section, the microstrip monopole antenna with various design parameters was constructed, and the numerical and experimental results of the input impedance and radiation characteristics are presented and discussed. Ansoft HFSS simulations [9] are used to optimize the design anda good agreement between the simulation and measurement is obtained.

The configuration of various antennas used for simulation studies are shown in Fig. 3. Voltage standing wave ratio (VSWR) characteristics for ordinary square monopole antenna [Fig. 3(a)], antenna with a pair of L-shaped slits in the ground plane [Fig. 3(b)], and the proposed antenna [Fig. 3(c)] structures are compared in Fig. 4.

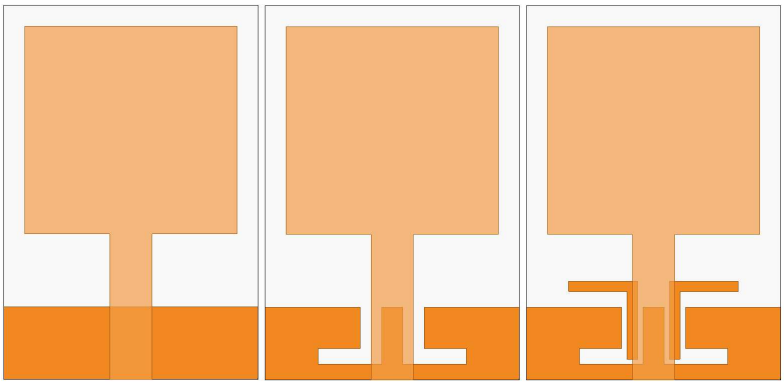


**Figure 3.** (a) Ordinary square monopole antenna, (b) antenna with a pair of L-shaped slits in the ground plane, and (c) the proposed antenna structure.

As shown in Fig. 4, the ordinary square monopole can provide the fundamental and next higher resonant radiation band at 4 and 8 GHz, respectively, in the absence of the L-shaped structures but in the proposed structure. The upper frequency bandwidth is significantly affected by using them. It is observed that by using these modified elements including L-shaped slits and parasitic structures, additional third (9.5 GHz), and fourth (13.7 GHz) resonances are excited and hence the bandwidth is increased [10–12].

In order to known the phenomenon behind these additional resonances performance, the simulated current distributions on the ground plane for the proposed antenna at 9.5 GHz, 13.7 GHz are presented

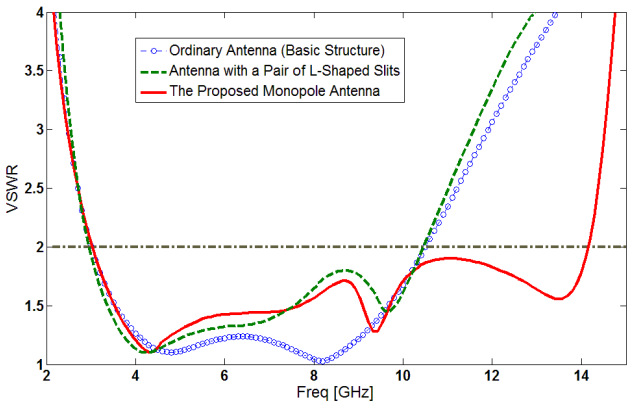


**Figure 4.** Simulated VSWR characteristics for the various structures shown in Fig. 2.

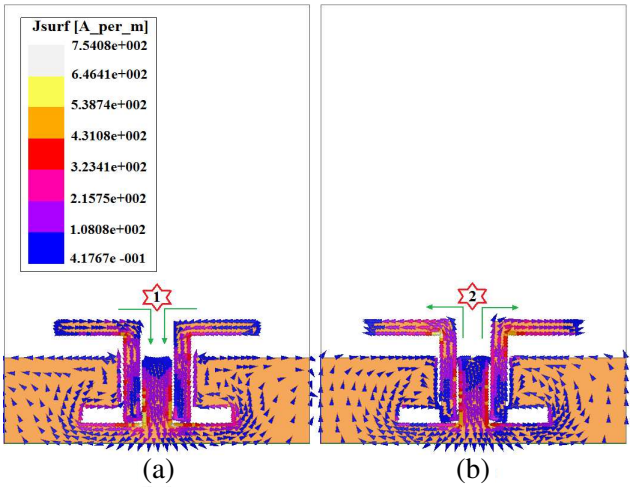


**Figure 5.** Simulated surface current distributions in the ground plane for proposed antenna at the additional resonances frequencies, (a) 9.5 GHz, (b) 13.7 GHz.

in Fig. 5. It can be observed in Fig. 5(a), that the current concentrated on the edges of the interior and exterior of the L-shaped slits at 9.5 GHz. As shown in Fig. 5(b) at the fourth resonance frequency the current flows are more dominant around of the inverted L-shaped parasitic structures. As seen in Figs. 5(a) and 5(b), the directions of surface currents are reversed in compared each other, which the antenna impedance changes at 9.5 and 13.7 GHz due to the resonant properties of the L-shaped slits and parasitic structures [13, 14].

The proposed antenna has a slightly higher efficiency rather than ordinary square antenna throughout the entire radiating band, which is mainly owing to the extra resonant properties. Results of the calculations using the software HFSS indicated that the proposed antenna features a good efficiency, being greater than 86% across the entire radiating band.

Measurement set-up of the proposed antenna for the VSWR, antenna gain and radiation pattern characteristics is shown in Fig. 6. As illustrated in Fig. 7, the proposed antenna was built and tested in the Antenna Laboratory at Microwave Technology Company (MWT). The VSWR characteristics of the

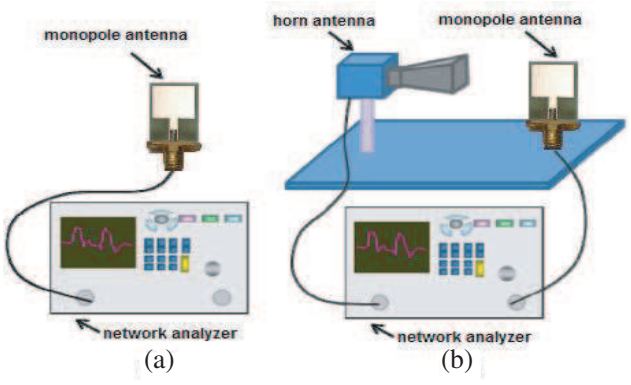


**Figure 6.** Measurement set-up of the proposed antenna, (a) VSWR, (b) antenna gain and radiation patterns.

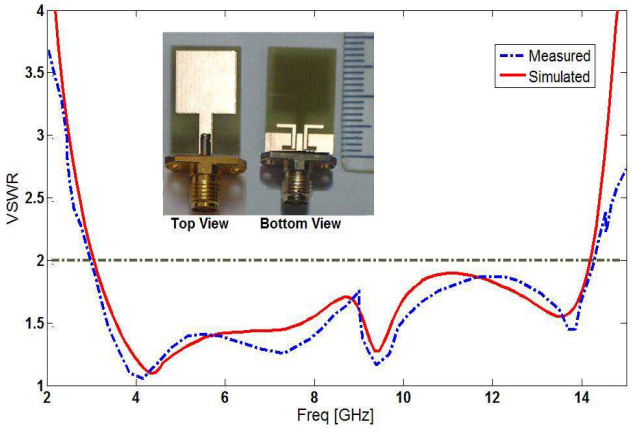


**Figure 7.** Measured and simulated VSWR characteristics of the proposed antenna.

antenna was measured using a network analyzer in an anechoic chamber. The radiation patterns have been measured inside an anechoic chamber using a double-ridged horn antenna as a reference antenna placed at a distance of 2 m. Also, two-antenna technique using a spectrum analyzer and a double-ridged horn antenna as a reference antenna placed at a distance of 2 m is used to measure the radiation gain in the $z$ axis direction ($x$-$z$ plane). The measured and simulated VSWR characteristics of the proposed antenna were shown in Fig. 7. The fabricated antenna has the frequency band of 2.95 to over 14.27 GHz.

However, as shown in Fig. 7, there exists a discrepancy between measured data and the simulated results. This discrepancy is mostly due to a number of parameters such as the fabricated antenna dimensions as well as the thickness and dielectric constant of the substrate on which the antenna is fabricated, the widge range of simulation frequencies. In a physical network analyzer measurement, the feeding mechanism of the proposed antenna is composed of a SMA connector and a microstrip line (the microstrip feed-line is excited by a SMA connector) whereas the simulated results are obtained using the Ansoft simulation software (HFSS), that in HFSS by default, the antenna is excited by a wave port that it is renormalized to a 50-Ohm full port impedance at all frequencies. In order to confirm the accurate return loss characteristics for the designed antenna, it is recommended that the manufacturing and measurement processes need to be performed carefully. Moreover, SMA soldering accuracy and FR4 substrate quality need to be taken into consideration.

The simulated and measured maximum gains of the antenna against frequency are illustrated in Fig. 8. The antenna gain has a flat property which increases by the frequency. As seen, the proposed antenna has sufficient and acceptable gain level in the operation bands.

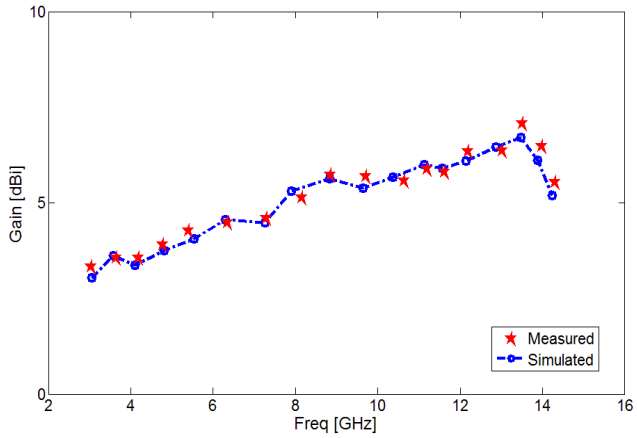


**Figure 8.** Measured and Simulated maximum gains of the proposed monopole antenna.

Figure 9 depicts the measured and simulated radiation patterns of the proposed antenna including the co-polarization and cross-polarization in the $H$-plane ($x$-$z$ plane) and $E$-plane ($y$-$z$ plane). It can be seen that quasi-omnidirectional radiation pattern can be observed on $x$-$z$ plane over the whole UWB frequency range, especially at the low frequencies. The radiation pattern on the $y$-$z$ plane displays a typical figure-of-eight, similar to that of a conventional dipole antenna. It should be noticed that the radiation patterns in $E$-plane become imbalanced as frequency increases because of the increasing effects of the cross polarization. The patterns indicate at higher frequencies, more ripples can be observed in both $E$- and $H$-planes owing to the generation of higher-order modes. The cross-polarization component also increases at higher frequencies due to the increased horizontal surface currents [15, 16].

In UWB microstrip antennas analysis, the transfer function is transformed to time domain by performing the inverse Fourier transform. Fourth derivative of a Gaussian function is selected as the transmitted pulse. Therefore the output waveform at the receiving antenna terminal can be expressed by convoluting the input signal and the transfer function. The input and received wave forms for the face-to-face and side-by-side orientations of the antenna are shown in Fig. 10.

It can be seen that the shape of the pulse is preserved in all the cases. Only due to being two notches, there is a bit distortion on received pulses which it was predictable. Using the reference and received signals, it becomes possible to quantify the level of similarity between signals [13].

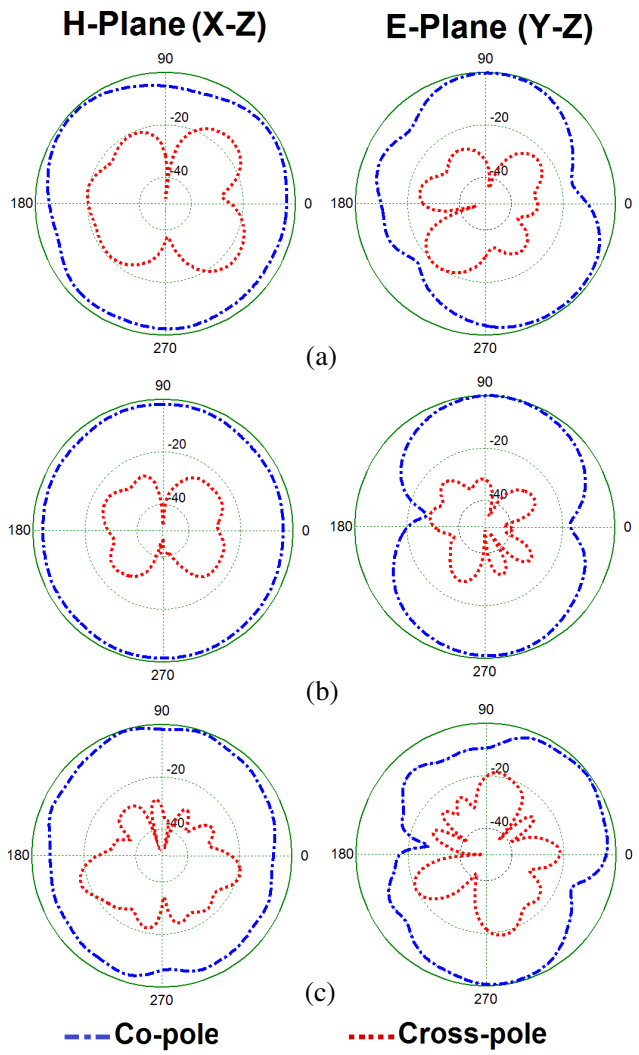


**Figure 9.** Measured radiation patterns of the proposed antenna, (a) 5.5 GHz, (b) 9.5 GHz, and (c) 13 GHz.

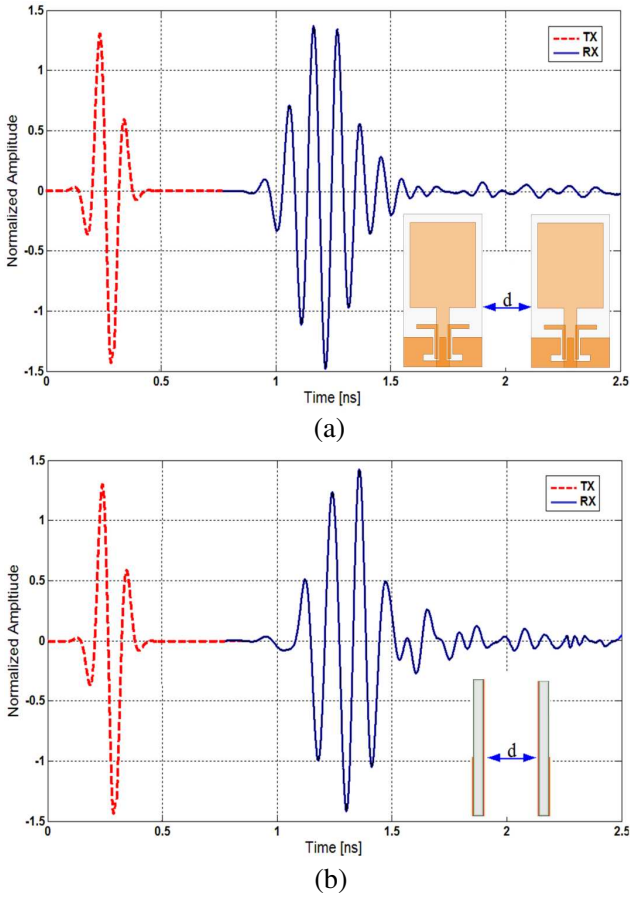


**Figure 10.** Transmitted and received pulses (a) side by side and (b) face to face.

In telecommunication systems, the correlation between the transmitted (TX) and received (RX) signals is evaluated using the fidelity factor (1).

$$F = \max_{\tau} \left| \frac{\int_{-\infty}^{+\infty} s(t) r(t-\tau)}{\sqrt{\int_{-\infty}^{+\infty} s(t)^2 dt \cdot \int_{-\infty}^{+\infty} r(t)^2 dt}} \right| \tag{1}$$

where $s(t)$ and $r(t)$ are the TX and RX signals, respectively. For impulse radio in UWB communications, it is necessary to have a high degree of correlation between the TX and RX signals to avoid losing the modulated information. However for most other telecommunication systems, the fidelity parameter is not that relevant. In order to evaluate the pulse transmission characteristics of the proposed UWB antenna with dual band-notches, two configurations (side-by-side and face-to-face orientations) were chosen. The transmitting and receiving antennas were placed in a $d = 250$ mm distance from each other.

As shown in Fig. 10, although the received pulses in each of two orientations are broadened, a

relatively good similarity exists between the RX and TX pulses. Using (1), the fidelity factor for the face-to-face and side-by-side configurations were obtained equal to 0.91 and 0.84, respectively. Values the fidelity factor show that the antenna imposes negligible effects on the transmitted pulses. The pulse transmission results are obtained using CST [17].

The radiating mechanism of the proposed antenna is more novel than was explained in previous works. The proposed structure is the combination of the monopole antenna with the dipole and slot antenna. In this study, the modified ground-plane structure is the combination of the monopole antenna and the slot antenna. By using the modified conductor-backed plane, the interaction of the two parts of the overall antenna is occurred. The embedding parasitic structure in the ground plane of the monopole antenna acts as a dipole antenna that can provide an additional current path. Also the entire back conducting plane could be part of the radiator, especially when operating at lower frequencies. As a result, the radiating mechanism may alter at various portions of the UWB band. The embedding conductor backed plane on the other side of the substrate of the monopole antenna acts as a dipole.

Table 2 summarizes the previous designs and the proposed antenna. As seen, the proposed antenna has a compact size with very wide bandwidth in compared the pervious works for microwave imaging applications. In addition, the proposed antenna has a good omni-directional radiation patterns with low cross-polarization level even at the higher and upper frequencies. As the proposed antenna has an ordinary square radiating patch without any slot and parasitic structures at top layer, in compared with previous multi-resonance UWB antennas, the proposed antenna displays a good omnidirectional radiation pattern even at lower and higher frequencies. Additionally, the antenna imposes negligible effects on the transmitted pulses and has a good antenna gain level in the operation bands.

**Table 2.** Comparison of previous designs with the proposed antenna.

| **Reference** | **Application** | **BW (VSWR $<$ 2)** | **Dimension (mm)** | **FBW (%)** | **Gain (dBi)** |
|---|---|---|---|---|---|
| **[10]** | Microwave Imaging Systems | (3.8–11.85 GHz) | $30 \times 30$ | 102% | not reported |
| **[11]** | Microwave Imaging Systems | (1.15–4.4 GHz) | $75 \times 75$ | 200% | $2 \sim 8$ |
| **[12]** | Microwave Imaging Systems | (4–9 GHz) | $30 \times 30$ | 76% | 2–6 |
| **[13]** | Microwave Imaging Systems | (2.97–12.83 GHz) | $12 \times 18$ | 124% | $3 \sim 6.1$ |
| **[14]** | Ultra Wideband Systems | (2.91–14.1 GHz) | $12 \times 18$ | 131% | 2.8–5.4 |
| **[15]** | Ultra Wideband Systems | (2.98–16.73 GHz) | $30 \times 30$ | 139 | not reported |
| **[16]** | Ultra Wideband Systems | (3.19–13.21 GHz) | $12 \times 18$ | 121% | $2.4 \sim 5.1$ |
| **This Work** | Microwave Imaging Systems | (2.95–14.27 GHz) | $12 \times 18$ | 132% | $3.3 \sim 6.5$ |

## 4. CONCLUSION

A compact monopole antenna with multi-resonance characteristic for use in microwave imaging system applications has been proposed. The fabricated antenna satisfies the VSWR $<$ 2 requirement from 2.95 to 14.27 GHz. In order to enhance bandwidth, two pairs of L-shaped slits and parasitic structures in the ground plane and hence much wider impedance bandwidth can be produced. The designed antenna has a simple configuration with an ordinary square radiating patch and small size of $12 \times 18\,\text{mm}^2$. Simulated and experimental results show that the proposed antenna could be a good candidate for circular cylindrical microwave imaging system applications.

## ACKNOWLEDGMENT

The author is thankful to Microwave Technology (MWT) Company staff for their beneficial and professional help (www.microwave-technology.com).

## REFERENCES


1. Fear, E. C., S. C. Hagness, P. M. Meaney, M. Okonieweski, and M. A. Stuchluy, "Enhancing breast tumor detection with near-field imaging," *IEEE Microw. Mag.*, Vol. 3, No. 1, 48–56, Mar. 2002.
2. Paulsen, K. D. and P. M. Meaney, "Nonactive antenna compensation for fixed-array microwave imaging — Part I: Model development," *IEEE Trans. Med. Imag.*, Vol. 18, No. 6, 496–507, Jun. 1999.
3. Bond, E. J., X. Li, S. C. Hagness, and B. D. Van Veen, "Microwave imaging via space-time beamforming for early detection of breast cancer," *IEEE Trans. Antennas Propag.*, Vol. 51, No. 8, 1690–1705, Aug. 2003.
4. Guillanton, E., J. Y. Dauvignac, C. Pichot, and J. Cashman, "A new design tapered slot antenna for ultra-wideband applications," *Microw. Opt. Technol. Lett.*, Vol. 19, No. 4, 286–289, 1998.
5. Chiappe, M. and G. L. Gragnani, "Vivaldi antennas for microwave imaging: Theoretical analysis and design considerations," *IEEE Trans. Instrum. Meas.*, Vol. 55, No. 6, 1885–1891, Dec. 2006.
6. Yun, X., E. C. Fear, and R. Johnston, "Broadband cross polarized bowtie antenna for breast cancer detection," *Proc. IEEE Antennas Propag. Soc. Int. Symp.*, Vol. 3, 1091–1094, Columbus, OH, Jun. 2003.
7. Shannon, C. J., E. C. Fear, and M. Okoniewski, "Dielectric filled slot line bowtie antenna for breast cancer detection," *Electron. Lett.*, Vol. 41, No. 7, 388–390, 2005.
8. Kanj, H. and M. Popovic, "Miniaturized microstrip-fed 'dark eyes' antenna for near-field microwave sensing," *IEEE Antennas Wireless Propag. Lett.*, Vol. 4, 397–401, 2005.
9. Ansoft High Frequency Structure Simulation (HFSS), Ver. 13, Ansoft Corporation, 2010.
10. Hossain, I., S. Noghanian, and S. Pistorius "A diamond shaped small planar ultra wide band (UWB) antenna for microwave imaging purpose," *Antennas and Propagation Society International Symposium*, 5713–5716, 2007.
11. Wu, B., Y. Ji, and G. Fang, "Design and measurement of compact tapered slot antenna for UWB microwave imaging radar," *The Ninth International Conference on Electronic Measurement & Instruments, ICEMI'2009*, 226–229, 2009.
12. Adnan, S., R. A. Abd-Alhameed, H. I. Hraga, I. T. E. Elfergani, J. M. Noras, and R. Halliwell, "Microstrip antenna for microwave imaging application," *PIERS Proceedings*, 431–434, Marrakesh, Morocco, Mar. 20–23, 2011.
13. Ojaroudi, N., M. Ojaroudi, and N. Ghadimi, "UWB omnidirectional square monopole antenna for use in circular cylindrical microwave imaging systems," *IEEE Antennas Wireless Propag. Lett.*, Vol. 11, 1350–1353, 2012.
14. Ojaroudi, M., S. Yzdanifard, N. Ojaroudi, and M. Nasser-Moghaddasi, "Small square monopole antenna with enhanced bandwidth by using inverted T-shaped slot and conductor-backed plane," *IEEE Trans. Antennas Propag.*, Vol. 59, No. 2, 670–674, Feb. 2011.
15. Ojaroudi, N. and N. Ghadimi, "UWB small slot antenna with WLAN frequency band-stop function," *Electron. Lett.*, Vol. 49, 1317–1318, 2013.
16. Ojaroudi, N., S. Amiri, and F. Geran, "Reconfigurable monopole antenna with controllable band-notched performance for UWB communications," *20th Telecommunications Forum (TELFOR)*, 1176–1178, Belgrade, Serbia, Nov. 20–22, 2012.
17. CST Microwave studio, *Computer Simulation Technology*, ver. 2008, Framingham, MA, 2008.